MOLECULAR AND CELLULAR BIOLOGY, Apr. 2006, p. 2511–2518 Vol. 26, No. 7
0270-7306/06/$08.00+0 doi:10.1128/MCB.26.7.2511–2518.2006

Hydrops Fetalis, Cardiovascular Defects, and Embryonic Lethality in Mice Lacking the *Calcitonin Receptor-Like Receptor* Gene

Ryan T. Dackor,[1,3] Kimberly Fritz-Six,[1] William P. Dunworth,[1,3] Carrie L. Gibbons,[1] Oliver Smithies,[2] and Kathleen M. Caron[1]*

Department of Cell & Molecular Physiology,[1] Department of Pathology and Laboratory Medicine,[2] and Curriculum in Genetics and Molecular Biology,[3] The University of North Carolina at Chapel Hill, Chapel Hill, North Carolina 27599

Received 30 August 2005/Returned for modification 19 September 2005/Accepted 3 January 2006

Adrenomedullin (AM) is a multifunctional peptide vasodilator that is essential for life. To date, numerous in vitro studies have suggested that AM can mediate its biological effects through at least three different receptors. To determine the in vivo importance of the most likely candidate receptor, calcitonin receptor-like receptor, a gene-targeted knockout model of the gene was generated. Mice heterozygous for the targeted *Calcrl* allele appear normal, survive to adulthood, and reproduce. However, heterozygote matings fail to produce viable *Calcrl*$^{-/-}$ pups, demonstrating that *Calcrl* is essential for survival. Timed matings confirmed that *Calcrl*$^{-/-}$ embryos die between embryonic day 13.5 (E13.5) and E14.5 of gestation. The *Calcrl*$^{-/-}$ embryos exhibit extreme hydrops fetalis and cardiovascular defects, including thin vascular smooth muscle walls and small, disorganized hearts remarkably similar to the previously characterized *AM*$^{-/-}$ phenotype. In vivo assays of cellular proliferation and apoptosis in the hearts and vasculature of *Calcrl*$^{-/-}$ and *AM*$^{-/-}$ embryos support the concept that AM signaling is a crucial mediator of cardiovascular development. The *Calcrl* gene targeted mice provide the first in vivo genetic evidence that CLR functions as an AM receptor during embryonic development.

Adrenomedullin (AM) is a potent peptide vasodilator that has been implicated in a wide variety of normal physiological processes including embryonic development (5), natriuresis (36), regulation of salt and water appetite (41, 48), cellular proliferation (7, 17, 49, 54), angiogenesis (11, 26), and antimicrobial defense (3). During many cardiovascular stresses such as pregnancy, septic shock, hypertension, and renal failure, plasma levels of AM are dramatically elevated and thought to provide a protective homeostatic response, diminishing adverse tissue remodeling and fibrosis associated with cardiovascular stress (16, 35, 42–44).

Our previous studies using a genetically engineered *AM* knockout mouse model have demonstrated an essential role for the *AM* gene in the development of cardiovascular tissues (5). Mice lacking the *AM* gene suffer from extreme hydrops fetalis and die at midgestation. The most obvious phenotype of *AM*$^{-/-}$ embryos is severe interstitial fluid accumulation and generalized edema. Closer evaluation of the *AM*$^{-/-}$ embryos also revealed developmental cardiovascular defects that include thin vascular smooth muscle walls and smaller hearts with thin compact zones and disorganized trabeculae (5). However, the cellular mechanisms underlying these embryonic cardiovascular defects remain unclear.

Since the identification of the AM peptide over 10 years ago (27), three putative receptors have been identified and suggested to mediate the biological effects of AM based on their ability to bind the peptide and elicit a cyclic AMP (cAMP) response to AM treatment in vitro. L1, originally cloned as an orphan receptor (10, 15), binds to AM with a K_D of 8.2×10^{-9} M and can mediate a cAMP response to AM when expressed in COS-7 cells (21). It is coexpressed with the AM peptide in most tissues (21) but is found in rat neonatal cardiac myocytes at significantly lower levels than the two other putative AM receptors (4). A second receptor, RDC-1, was originally identified as a receptor for the AM-related peptide, calcitonin gene-related peptide (CGRP), but also binds to AM with a K_D of 1.9×10^{-7} M and mediates a dose-dependent cAMP response to AM when expressed in COS-7 cells (22). A third receptor, commonly referred to as the calcitonin receptor-like receptor (designated CRLR) and now usually referred to as the calcitonin-like receptor (CLR), was cloned independently by several groups (1, 14) but subsequently failed to produce consistent expression, binding, and functional results with CGRP or AM (1, 9, 12, 14, 45). Several recent studies have also failed to support the role of either L1 or RDC-1 as AM receptors (19, 25, 32, 39).

Most recently, the identification of a novel class of G-protein-coupled receptor (GPCR) activity-modifying proteins (receptor activity-modifying proteins are designated RAMPs) and their association with CLR has helped to elucidate the most likely mechanism through which the AM peptide transduces its signal. Briefly, McLatchie et al. demonstrated that association with RAMP1 made CLR bind preferentially to CGRP, while association of CLR with RAMP2 or RAMP3 made it bind to AM (39). This novel role of the RAMPs in GPCR cell signaling implies that the spatial and temporal expression of RAMPs dictates the presence and function of CLR as an AM receptor or a CGRP receptor and helps clarify some of the past confusion regarding AM signaling. However, no in vivo genetic studies to substantiate the identity of CLR as a functional AM recep-

* Corresponding author. Mailing address: Department of Cell & Molecular Physiology, CB #7545, 6330 MBRB, 103 Mason Farm Rd., The University of North Carolina at Chapel Hill, Chapel Hill, NC 27599. Phone: (919) 966-5215. Fax: (919) 966-5230. E-mail: kathleen_caron@med.unc.edu.

tor have been performed, despite great interest in the role of the peptide during embryonic development and the possibility that modulating AM function might prove valuable for the treatment of cardiovascular disease.

In this paper, we used gene targeting in embryonic stem cells to generate and characterize mice that are deficient for the gene which encodes CLR. We find that although *Calcrl*$^{+/-}$ mice have no overt phenotypic defects, the *Calcrl* gene is essential for survival, since no *Calcrl*$^{-/-}$ pups have ever been born from heterozygote matings. Significantly, the embryonic lethal phenotype of *Calcrl*$^{-/-}$ mice is remarkably similar to the phenotype we previously observed for *AM*$^{-/-}$ mice, including hydrops fetalis and developmental abnormalities in cardiovascular tissues (5). More detailed characterization of the growth properties of *Calcrl*$^{-/-}$ and *AM*$^{-/-}$ vasculature and hearts has further confirmed an essential role for this signaling pathway in the growth and proliferation of the embryonic cardiovascular system.

MATERIALS AND METHODS

Construction of the *Calcrl* targeting vector. To generate a *Calcrl* knockout targeting vector, a 129S6/SvEv genomic library was screened for phage clones containing the 5′ portion of the *Calcrl* gene. A genomic clone consisting of approximately 11.5 kb and containing exons 3 through 9 of the *Calcrl* gene was used to isolate and clone a 5′ short arm and 3′ long arm of homology into a gene targeting vector (OSdupdel), which contains multiple cloning sites flanking a phosphoglycerate kinase-neomycin cassette and also includes a herpes simplex virus-thymidine kinase cassette. The 5.0-kb long arm of homology, which includes exons 7, 8, and 9, was isolated and subcloned with HindIII and XhoI restriction sites endogenous to the gene locus. The 1.3-kb short arm of homology containing exon 4 was generated by PCR using the genomic phage clone as a template and oligonucleotide sequences that correspond to genomic sequences 5′-GGAAATTAGATTTTCAAGGGGTG-3′ and 5′-GGCCTTTAAACTGTG AGCAAAG-3′. The short arm was inserted into the targeting vector by blunt ligation, and the final targeting vector was linearized with NotI (Fig. 1a).

Generation of *Calcrl*$^{+/-}$ ES cells and *Calcrl*$^{-/-}$ mice. Standard gene targeting methods were utilized to generate embryonic stem (ES) cells and mice lacking CLR (30). Briefly, 129S6/SvEv-TC-1 embryonic stem cells were electroporated with the linearized targeting vector shown in Fig. 1a. After the application of positive (G418) and negative (ganciclovir) selection, a positive ES cell clone was identified by PCR from >800 selected clones. For PCR-based screening of targeted ES cells, we used three primers depicted in Fig. 1a: primer 1, 5′-GTG ATTTGAGTCTGGAGA-3′; primer 3, 5′-GAAATGTGCTGTATGTTCAAG-3′; and primer 4, 5′-TGGCGGACCGCTATCAGGAC-3′. Male chimeric mice that transmitted the targeted allele were bred to 129S6/SvEv females to establish an isogenic colony. To isolate *Calcrl*$^{-/-}$ embryos, heterozygote *Calcrl*$^{+/-}$ breedings were established, and the day of the vaginal plug was considered embryonic day 0.5 (E0.5). For routine PCR-based genotyping of mice, we used a three-primer strategy in which primer 2 (5′-GCTATGCTTTGTTTTCTGACA-3′) and primer 3 amplified the wild-type (WT) allele, while primer 2 and primer 4 amplified the targeted allele.

Generation of *AM*$^{-/-}$ mice. The generation, genotyping, and characterization of mice with a targeted deletion of the *AM* gene have been previously described (5).

Gene expression analysis. *Calcrl* gene expression was analyzed by real-time quantitative reverse transcription-PCR with the Mx3000P Real-Time PCR machine from Stratagene. Primers for *Calcrl* amplification were 5′-CAAGATCAT GACGGCTCAATA-3′ and 5′-CGTCATTCCAGCATAGCCAT-3′. The probe sequence for *Calcrl* detection was 5′-FAM-CATGCAGGACCCCATTCAACA AGCAT-TAMRA-3′, where FAM is 6-carboxyfluorescein and TAMRA is 6-carboxy-tetramethylrhodamine. β-Actin served as an internal control for all reactions. The primers used for β-actin amplification were 5′-CTGCCTGACGGCC AAGTC-3′ and 5′-CAAGAAGGAAGGCTGGAAAAGA-3′. The probe sequence for β-actin detection was 5′-tetrachloro-6-carboxyfluorescein-CACTATTGGCAAC GAGCGGTTCCG-TAMRA-3′. RNA was isolated from E13.5 embryos with TRIzol reagent (GIBCO/BRL), DNase treated, and purified with an RNeasy Mini Kit (QIAGEN). A total of 200 ng of total RNA was used in each reaction mixture. The $\Delta\Delta C_T$ method (33) was used to determine the relative levels of *Calcrl* expression and shown as a percentage of the wild type. All assays were repeated three times, each with duplicates.

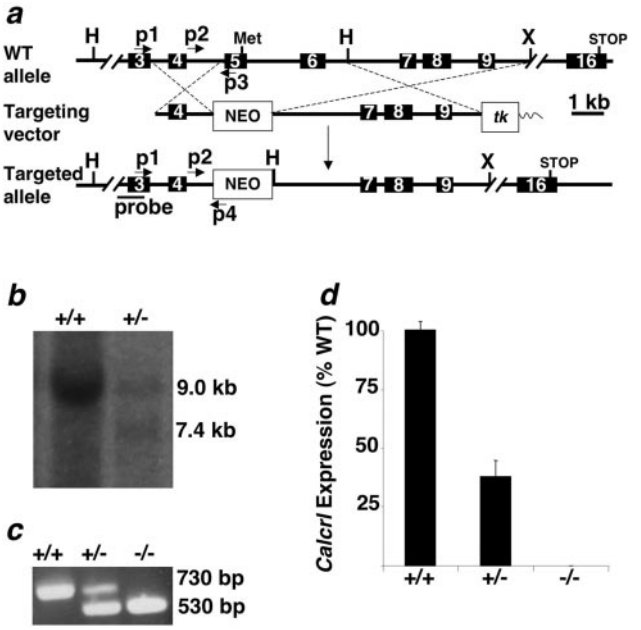

FIG. 1. Generation of *Calcrl*$^{-/-}$ animals by homologous recombination. (a) Strategy to disrupt the *Calcrl* gene. (Top) Endogenous wild-type allele. (Middle) Targeting vector. (Bottom) Targeted allele following homologous recombination. Primer locations for PCR (p1, p2, p3, and p4) are shown by arrows. The location of the probe used for the Southern-based detection strategy is indicated by a labeled line (probe). The targeting vector plasmid sequence is indicated by a thin wavy line. Restriction sites: H, HindIII; X, XhoI. The initiator methionine and terminator codons are indicated as Met and STOP. (b) Detection of targeted ES cells by Southern blot analysis. Digestion of genomic DNA with HindIII results in a 9.0-kb fragment for the WT allele and a 7.4-kb fragment for the targeted allele when probed with the fragment depicted in panel a. (c) Primers depicted in panel a were used to amplify genomic DNA from embryos. (d) Measurement of *Calcrl* expression from total RNA extracts by real-time quantitative reverse transcription-PCR. The relative quantity of *Caclrl* RNA in *Calcrl*$^{+/-}$ and *Calcrl*$^{-/-}$ embryos is represented as a percentage of total *Calcrl* RNA in WT embryos. Error bars represent standard errors of the mean.

Histology. For histological analyses, embryos were dissected from the uterus at the desired stage of gestation, fixed in 4% paraformaldehyde, dehydrated, and embedded in paraffin wax. Sections (5 μm thick) were mounted on slides for subsequent hematoxylin and eosin (H&E), anti-α-smooth muscle actin (anti-α-SMA), bromodeoxyuridine (BrdU), or terminal deoxynucleotidyltransferase-mediated dUTP-digoxigenin nick end labeling (TUNEL) staining.

Anti-PECAM staining. Tissues were fixed in 4% paraformaldehyde in phosphate-buffered saline (PBS) overnight. Tissues were then cryoprotected with 30% sucrose in PBS overnight, embedded in OCT (Tissue-Tek) and cryosectioned at 10 μm. Sections were rehydrated in PBS, quenched in 50 mM NH_4Cl in PBS, permeabilized with 0.2% Triton X-100–PBS, and blocked in 3% bovine serum albumin–1% fetal bovine serum in PBS. Sections were incubated with anti-platelet endothelial cell adhesion molecule 1 (anti-PECAM-1; catalogue no. 550274; BD Pharmingen) overnight at 4°C. After being washed with Tris-buffered saline–Tween (TBST) and PBS, sections were incubated with a Cy3-labeled donkey anti-rat secondary antibody (code no. 712-165-150, Jackson ImmunoResearch) for 2 h at room temperature. Sections were then washed with TBST and PBS and mounted for imaging. Images were acquired on a Nikon E800 microscope with a Hammamatsu ORCA-ER charge-coupled device camera with Metamorph software (Molecular Devices Corp.) and processed with Photoshop.

Anti-α-SMA staining. Paraffin sections were deparaffinized, rehydrated, and subsequently placed in 0.3% H_2O_2 in methanol for 15 min to block endogenous peroxidase activity. Sections were then rinsed in distilled H_2O and permeabilized

in 3% bovine serum albumin with 0.2% Triton X-100 in PBS. After being washed in PBS, specimens were incubated with α-smooth muscle actin (α-SMA) (catalogue no. A2547; Sigma) antibody for 1 h at room temperature. Sections were then washed with TBST and PBS and incubated with an horseradish peroxidase-labeled goat anti-mouse secondary antibody (catalogue no. 12-349; Upstate) for 90 min at room temperature. After being washed with TBST and PBS, the peroxidase reaction was visualized with diaminobenzidine-hydrogen peroxide (product no. 34065; Pierce), counterstained with 1% methyl green, and mounted for imaging. Images were acquired on a Nikon FXA microscope and processed with Photoshop.

Cell proliferation assay. To label proliferating cells, pregnant mice received a single intraperitoneal injection of BrdU (B9285; Sigma), using 100 mg of BrdU per kg of body weight. One hour after injection, pregnant females were euthanized by cervical dislocation, and embryos were prepared for histology as described above. BrdU was detected with the BrdU Staining kit from Zymed (catalogue no. 93–3943). Images were collected using a Leica MZ 16 FA dissecting microscope, and the number of BrdU-positive cells was quantified as the number of BrdU-positive cells per area with Image J software.

TUNEL cell death assay. Apoptotic cells were identified in 5-μm paraffin-embedded sections with the ApopTag Fluorescein *In Situ* apoptosis detection kit (Chemicon) according to the manufacturer's protocol. Images were acquired on a Nikon E800 microscope with a Hammamatsu ORCA-ER charge-coupled device camera with Metamorph software (Molecular Devices Corp.) and processed with Photoshop.

Statistics. Statistical analyses were performed with a Student *t* test with unequal variance.

Experimental animals. All experiments were approved by the Institutional Animal Care and Use Committee of The University of North Carolina at Chapel Hill.

RESULTS

Generation of mice lacking the *Calcrl* gene. Mice in which exons 5 and 6 of the *Calcrl* gene were deleted by homologous recombination were generated using the targeting strategy shown in Fig. 1a. The disrupted allele, which lacks the *Calcrl* translation start site, was detected by Southern blot analysis using a genomic probe fragment located outside the areas of homology (Fig. 1b) and by PCR (Fig. 1c). To confirm that the gene targeting effectively disrupted transcription of the *Calcrl* gene, quantitative reverse transcription-PCR for *Calcrl* RNA was performed on total RNA isolated from whole embryos. As expected, $Calcrl^{+/-}$ embryos expressed approximately half of wild-type *Calcrl* RNA levels (38.2%; $P < 0.0001$ versus the wild type) while $Calcrl^{-/-}$ embryos had no detectable levels of *Calcrl* RNA, thus confirming complete loss of *Calcrl* expression in knockout embryos (Fig. 1d).

***Calcrl*$^{-/-}$ mice die at midgestation with extreme hydrops fetalis.** Mice heterozygous for the targeted *Calcrl* allele appeared normal at birth, survived to adulthood, and reproduced. However, the breeding of $Calcrl^{+/-}$ mice failed to produce any viable $Calcrl^{-/-}$ offspring, demonstrating that the *Calcrl* gene is essential for survival. Timed matings between $Calcrl^{+/-}$ mice revealed that, although the homozygous null $Calcrl^{-/-}$ embryos were indistinguishable from their wild-type littermates at E11.5 (data not shown), by E12.5 the $Calcrl^{-/-}$ embryos were readily distinguishable from their $Calcrl^{+/+}$ and $Calcrl^{+/-}$ littermates by the presence of generalized, interstitial edema (Fig. 2a). The edema formation rapidly progressed, so that by day E13.5 all $Calcrl^{-/-}$ embryos suffered from extreme hydrops fetalis (Fig. 2b) with an associated in utero mortality rate of approximately 50%. By E14.5, all $Calcrl^{-/-}$ embryos examined were dead. We note that our previous studies with $AM^{-/-}$ mice (5) revealed a similar type of generalized edema; however, the onset of the edema occurred 24 h later in gestation at E13.5.

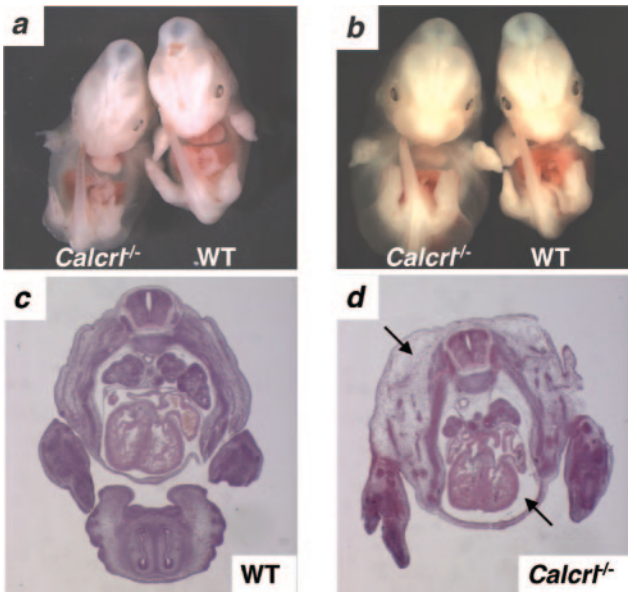

FIG. 2. $Calcrl^{-/-}$ embryos have massive generalized edema. (a) Generalized edema is observed throughout the entire body in $Calcrl^{-/-}$ embryos at E12.5. (b) By E13.5, the generalized edema in $Calcrl^{-/-}$ embryos has progressed to severe hydrops fetalis. (c and d) H&E stain of transverse sections through E13.5 WT (c) and $Calcrl^{-/-}$ (d) embryos. The thoracic cavity and interstitial tissues are filled with fluid and distended (d, arrows). Magnification, ×1.

Histological examination of $Calcrl^{-/-}$ embryos at E13.5 revealed distended skin, due to fluid accumulation in the interstitial space and a distended fluid-filled thoracic cavity (Fig. 2d; Fig. 3e and f). We did not observe any significant hemorrhage in the hydropic $Calcrl^{-/-}$ embryos, suggesting that the blood vascular system remained structurally intact.

***Calcrl*$^{-/-}$ embryos have thin vascular smooth muscle walls.** Numerous reports generated from in vitro experiments have shown that AM has either a negative or positive effect on vascular smooth muscle cell proliferation (17, 20, 49, 55). Therefore, we used our in vivo genetic model to determine the role of AM signaling in the vascular smooth muscle cell layer of the developing aorta.

Histological comparison of the descending aorta revealed significantly fewer vascular smooth muscle cells in $Calcrl^{-/-}$ knockout embryos than in their wild-type littermates at gestational days E12.5 and E13.5 (Fig. 3b, c, e, and f). This difference in vascular muscle wall thickness between $Calcrl^{-/-}$ and wild-type littermates was not apparent 1 day earlier in gestation at E11.5 (Fig. 3a and d).

The percentage of BrdU-positive cells in the vascular smooth muscle cell layer of the descending aorta of E12.5 embryos was quantified to determine the effects of CLR deletion on cellular proliferation (Fig. 3g). We found a significant reduction in the percentage of BrdU-positive cells in the vessel walls of $Calcrl^{-/-}$ embryos compared to wild-type littermates (17.67% ± 1.17% for $Calcrl^{-/-}$ versus 27.64% ± 2.01% for the wild type; $P \leq 0.005$).

To establish that the reduction in vascular smooth muscle wall thickness in $Calcrl^{-/-}$ embryos was not affected by abnormal smooth muscle cell differentiation or defects in endothelial

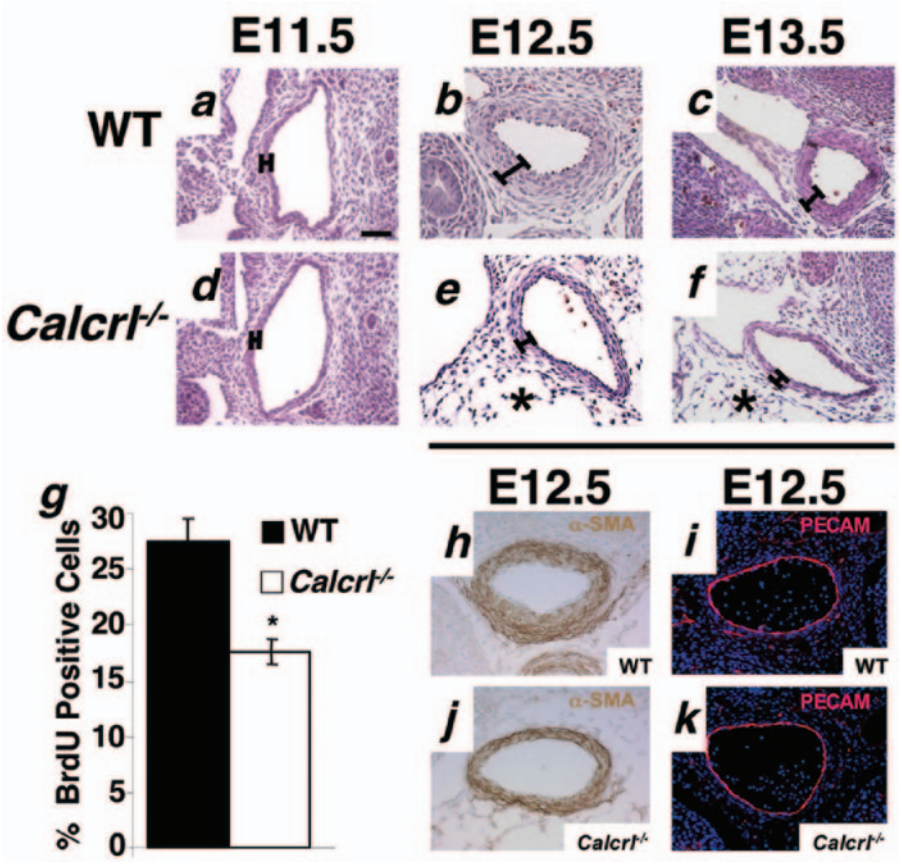

FIG. 3. *Calcrl*$^{-/-}$ embryos have thin arterial walls due to reduction in vascular smooth muscle cell proliferation. (a to f)Transverse sections through the descending aorta of wild-type and *Calcrl*$^{-/-}$ embryos at E11.5, 12.5, and 13.5 were stained with H&E. The thickness of the vessel walls at E11.5 is similar in wild-type and *Calcrl*$^{-/-}$ sections. However, by E12.5 and E13.5, the vascular walls are thinner in *Calcrl*$^{-/-}$ mice (approximately three cells thick) compared to wild-type controls (approximately six cells thick). Asterisks indicate the accumulation of interstitial edema in *Calcrl*$^{-/-}$ embryos. The percentage of proliferating, BrdU-positive cells in the aortic walls of *Calcrl*$^{-/-}$ mice is significantly less than in those of wild-type controls (g). (h and j) Vascular smooth muscle cells in wild-type and *Calcrl*$^{-/-}$ aortas stain positive for α-SMA. (i and k) Anti-PECAM staining shows that wild-type and *Calcrl*$^{-/-}$ aortas have normal endothelial patterning. Magnification, ×10. Scale bar, 50 μm.

patterning, we performed immunohistochemistry using antibodies against a smooth muscle marker, α-SMA, and an endothelial marker, PECAM. As shown in Fig. 3 h and j, the aortic vascular smooth muscle cells of *Calcrl*$^{-/-}$ mice, like those of their wild-type counterparts, are positive for α-SMA, demonstrating normal vascular smooth muscle cell differentiation. Anti-PECAM staining also revealed a complete and well-formed endothelial lining in the aorta, demonstrating that endothelial tube formation and the final patterning of the endothelial lining of the large vessels is unaffected in the major arteries of *Calcrl*$^{-/-}$ mice compared to wild-type embryos (Fig. 3i and k).

***Calcrl*$^{-/-}$ embryos have small and disorganized hearts.** Transverse sections through the embryonic hearts at E11.5 revealed no obvious differences between *Calcrl*$^{-/-}$ and wild-type mice (Fig. 4a and d). However, by E12.5 (Fig. 4b and e) the *Calcrl*$^{-/-}$ embryos had significantly smaller hearts than their wild-type littermates. By E13.5 (Fig. 4c and f) the overall heart size of the *Calcrl*$^{-/-}$ embryonic heart was approximately two-thirds the size of the wild-type littermate heart. The atria, mitral and tricuspid valves, endocardial cushion, and ventricular septum appeared normal at all gestational ages (Fig. 4). Higher magnification of the left ventricle showed that at E12.5 and E13.5 the compact zone of *Calcrl*$^{-/-}$ hearts appeared thin and discontinuous (Fig. 5f to h) compared to wild-type controls (Fig. 5b to d). The myocardium also had a generally disorganized structure, and the chamber appeared crowded (Fig. 5g and h). Immunohistochemical staining to characterize the presence and location of cardiomyocytes (α-actinin), endocardial cells (PECAM), and proliferating myofibroblasts (α-smooth muscle actin) revealed no obvious abnormalities in *Calcrl*$^{-/-}$ hearts, compared to wild-type control hearts (data not shown).

Decreased cellular proliferation in *Calcrl*$^{-/-}$ and *AM*$^{-/-}$ hearts. Based on our observation of smaller heart size and the fact that both AM and CGRP peptides had previously been shown to mediate cell growth, proliferation, and survival in a variety of different tissues (2, 17, 37, 57), we evaluated the extent of cell proliferation and apoptosis in developing *Calcrl*$^{-/-}$ and *AM*$^{-/-}$ hearts at various gestational stages. Using the incorporation of BrdU as a measure of cell proliferation, we found no significant difference in the amount of proliferation in the ventricles of E11.5 *Calcrl*$^{-/-}$ embryos compared to that in wild-type littermates (101 ± 3.25 for *Calcrl*$^{-/-}$ versus 101.6 ± 4.14 for wild-type; $P = 0.927$) (Fig. 6a). In contrast, by E12.5

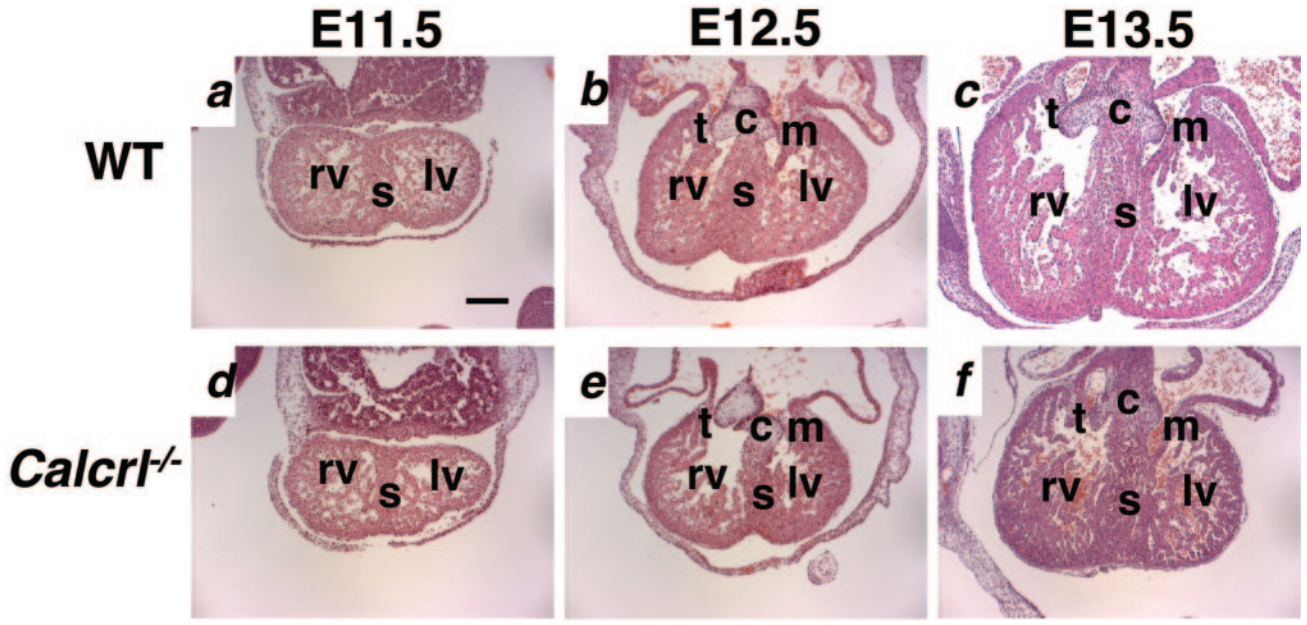

FIG. 4. *Calcrl*$^{-/-}$ embryos have developmental heart defects. Transverse sections through the hearts of wild-type and *Calcrl*$^{-/-}$ embryos at E11.5, 12.5, and 13.5 were stained with H&E. (a and d) At E11.5, the overall heart size is similar in both wild-type and *Calcrl*$^{-/-}$ embryos. (b and e) At E12.5, the overall heart size in the *Calcrl*$^{-/-}$ embryo is smaller than that of its wild-type littermate. (c and f) At E13.5, the overall heart size in the *Calcrl*$^{-/-}$ embryo is approximately two-thirds the size of that of its wild-type littermate. c, endocardial cushion; s, septum; t, tricuspid valve; m, mitral valve; rv, right ventricle; lv, left ventricle. Magnification, ×4. Scale bar, 200 μm.

we found a significant reduction in the total number of BrdU-positive cells in the ventricles of *Calcrl*$^{-/-}$ embryos compared to wild-type littermates (80.45 ± 6.21 for *Calcrl*$^{-/-}$ versus 111.66 ± 4.29 for the wild type; $P \leq 0.005$) (Fig. 6a). Similarly, E13.5 *AM*$^{-/-}$ embryos showed a significant reduction in BrdU-positive cells in the ventricles compared to wild-type littermate controls (58.12 ± 2.51 for *AM*$^{-/-}$ and 82.52 ± 8.87 for the wild type; $P < 0.05$) (Fig. 6b).

Increased apoptosis in *Calcrl*$^{-/-}$ and *AM*$^{-/-}$ hearts. Staining for apoptotic cells by TUNEL also revealed remarkable differences between the development of *Calcrl*$^{-/-}$ *and AM*$^{-/-}$ hearts compared to those of wild-type littermates. At E11.5, we found no obvious differences in the overall number of apoptotic cells which are normally present in the developing endocardial cushion, ventricular septum, and ventricular apex of the heart (data not shown). Comparison of TUNEL staining in other organs of *Calcrl*$^{-/-}$ and wild-type littermates at E13.5 also revealed no significant difference in the number of apoptotic cells in the lung, dorsal root ganglia, or the central canal of the spinal cord and only a slight increase in the liver (data

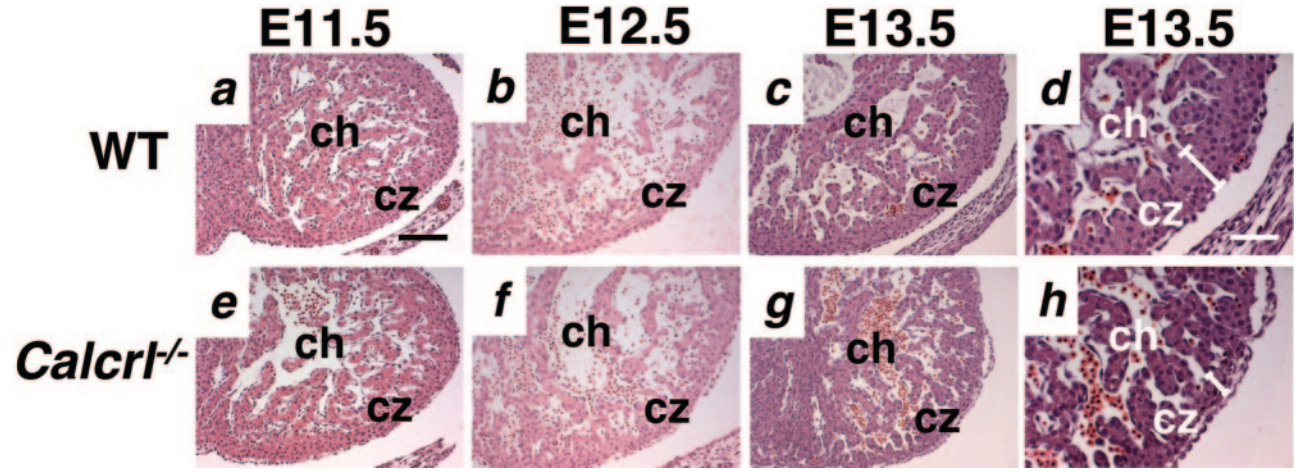

FIG. 5. *Calcrl*$^{-/-}$ embryos show thin and disorganized compact zones of the heart. Transverse sections through the hearts of wild-type and *Calcrl*$^{-/-}$ embryos at E11.5, 12.5, and 13.5 were stained with H&E. The compact zone in wild-type and *Calcrl*$^{-/-}$ embryos at E11.5 (a and e) and E12.5 (b and f) is similar in thickness and cellular organization. At E13.5 (c and g), the compact zone is thinner in the *Calcrl*$^{-/-}$ embryo. Higher magnification (d and h) reveals a discontinuous and convoluted organization of the compact zone in the *Calcrl*$^{-/-}$ section. ch, chamber; cz, compact zone. Magnification, ×10 (a to c and e to g); ×20 (d and h). Scale bar, 100 μm (a to c and e to g); 50 μm (d and h).

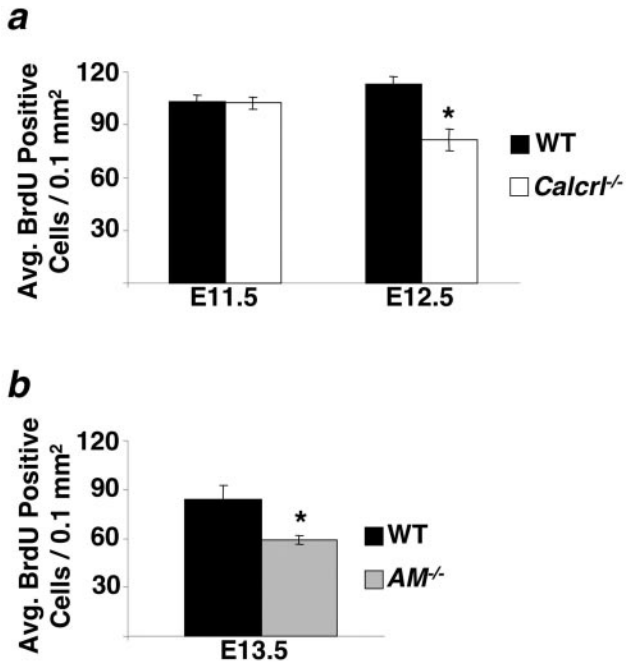

FIG. 6. *Calcrl*$^{-/-}$ and *AM*$^{-/-}$ embryos have defects in cardiac cell proliferation. The proliferation index of cardiac cells was determined as the number of BrdU-positive cells per total area in transverse heart sections. (a) No significant difference was found between wild-type and *Calcrl*$^{-/-}$ embryos at E11.5. However, at E12.5 the proliferation index was significantly lower in *Calcrl*$^{-/-}$ embryos than in wild-type controls. (b) The proliferation index of *AM*$^{-/-}$ embryos at E13.5 is significantly lower than that of wild-type littermates.

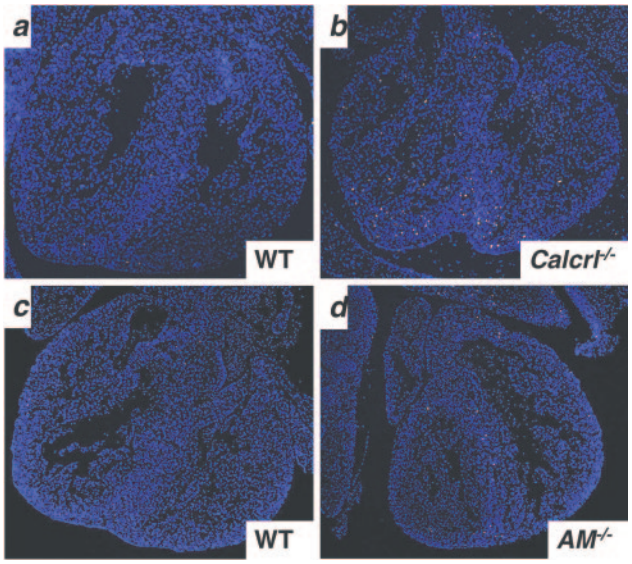

FIG. 7. *Calcrl*$^{-/-}$ and *AM*$^{-/-}$ embryos at E13.5 have increased levels of cardiac apoptosis. Typical pictures of TUNEL-stained transverse sections. (a) The number of TUNEL-positive cells is greater in *Calcrl*$^{-/-}$ (b) and *AM*$^{-/-}$ (d) hearts than in hearts of wild-type littermates (a and c).

not shown). However, by E13.5 we found a marked increase (approximately six times more than the wild type) in the number of TUNEL-positive cells throughout the heart, particularly in the ventricular apex, endocardial cushion, and septum of *Calcrl*$^{-/-}$ and *AM*$^{-/-}$ embryos compared to control littermates (Fig. 7).

DISCUSSION

We used gene targeting in embryonic stem cells to generate and characterize mice that are deficient for the gene that encodes one of the three putative AM receptors, CLR. Our most significant finding is that the *Calcrl* gene is essential for survival, since *Calcrl*$^{-/-}$ mice die in utero at midgestation. Significantly, the embryonic lethal phenotype of the *Calcrl*$^{-/-}$ mice is almost indistinguishable from the phenotype we previously characterized for mice carrying a targeted deletion of the AM peptide (5). These shared phenotypes include severe generalized edema, developmental abnormalities in cardiovascular tissues that consist of reduced vascular smooth muscle cell development in the large arteries, and a small overall heart size with a thin and discontinuous compact zone. Although biochemical studies have identified at least three putative receptors for AM peptide signaling, the remarkable similarity between the phenotypes observed for these two knockout models provides compelling genetic and in vivo evidence that CLR is the primary receptor through which AM peptide acts during embryonic development. However, our results do not exclude the possibility that L1 or RDC1 or both also contribute to the function of AM at the same stage of life.

Another recent description of a gene-targeted mouse model by Czyzyk et al. also provides additional compelling support for our conclusion that disruption of AM signaling during embryonic development results in the consistent phenotype we describe. In their study, the authors show that deletion of the gene that encodes peptidylglycine α-amidating monooxygenase, an enzyme that serves as the sole source of peptide amidation in the mouse, results in embryonic lethality, edema, and cardiovascular defects that phenocopy the *AM* and *Calcrl* knockout models. Since amidation of AM peptide is required for its biological activity, the authors conclude that lack of amidation results in loss of AM function, presumably by reducing its ability to bind to its receptor(s), with a resulting phenotype that is strikingly similar to that seen with *AM* knockout embryos. Because several mouse models for deletion of genes that encode other amidated peptides exist in which similar phenotypes are not observed, it is likely that inactivation of AM signaling in peptidylglycine α-amidating monooxygenase mutants is the primary cause of the phenotype observed (8). Taken together, the description of a similar phenotype for three separate knockout mouse models demonstrates that abnormal cardiovascular development and generalized edema can be expected when AM signaling is disrupted during embryonic development.

The only significant difference we found between the CLR knockout and AM peptide knockout models is the timing of phenotypic onset: the edema and cardiovascular defects appeared 24 h earlier in the *Calcrl*$^{-/-}$ knockout embryos (E12.5) than in the *AM*$^{-/-}$ knockout embryos (E13.5) (5). Given the recent finding that RAMPs determine the ligand binding affinity for CLR to either the CGRP peptide or the AM peptide, the most likely explanation for the difference in time of phe-

notypic onset is that $Calcrl^{-/-}$ mice have lost the ability to transduce signal for both AM and CGRP peptides by virtue of losing a shared GPCR. The *AM* knockout mice may survive a while longer because they still have CGRP peptide signaling, which is probably absent in the more severely affected $Calcrl^{-/-}$ mice. However, it is clear that CGRP signaling is not essential for survival, since CGRP peptide knockout mice develop normally and survive to adulthood with only modest defects in blood pressure regulation and sympathetic nervous activity (13, 34, 47, 58). In addition, our experiments do not rule out the possibility that CLR, perhaps in association with different RAMPs, may bind and mediate the function of other unidentified peptide ligands. Thus, the precise reason for the difference in gestational phenotypic onset between the $Calcrl^{-/-}$ and $AM^{-/-}$ mice remains an ongoing area of investigation.

The cause of edema in the $Calcrl^{-/-}$ and $AM^{-/-}$ mice also requires further investigation. Embryonic lethality due to cardiovascular defects in genetically engineered murine models is sometimes associated with embryonic edema (6, 31, 38, 46, 50). However, the edema is usually mild, localized to the subcutaneous region, and accompanied by hemorrhage and/or a blood-filled liver. In contrast, two recent reports demonstrate that generalized, interstitial edema similar to that seen with the $Calcrl^{-/-}$ and $AM^{-/-}$ knockouts is caused by abnormalities in or failure of lymphatic vessel development (23, 56). Given the role of AM as an angiogenic factor, it is possible that a lack of AM signaling by genetic deletion of either the AM peptide or the CLR results in lymphatic defects that cause severe and generalized hydrops fetalis. Current data are not yet sufficient to conclude the cause of edema in our mice.

It is well appreciated that AM peptide can differentially affect the growth properties of various cell types (2, 17, 37, 57). For example, while AM can inhibit apoptosis of cardiomyocytes (24, 51), it can also promote endothelial and vascular smooth muscle cell proliferation (17, 40). The effects of enhanced or reduced AM signaling on cells of the cardiovascular system are of particular interest, since AM peptide levels dramatically increase in patients suffering from many cardiovascular conditions, including congestive heart failure (18), hypertension (29), myocardial infarction (28), and cardiac hypertrophy (52), and may provide protection against the development of adverse tissue remodeling and fibrosis associated with cardiovascular stress (43, 44, 53). Our data provide the first in vivo, genetic evidence that the *AM* and *CLR* genes allow transduction of essential signals during development that positively mediate the growth and proliferation of vascular smooth muscle cells and cardiac cells while concurrently negatively influencing cardiac cell apoptosis.

In conclusion, our studies using a genetically engineered knockout model for the *Calcrl* gene demonstrate an essential role for the CLR GPCR during embryonic cardiovascular development. The remarkable similarity between the $Calcrl^{-/-}$ and $AM^{-/-}$ embryonic phenotypes leads us to conclude that CLR is the predominant receptor mediating AM signaling during development.

ACKNOWLEDGMENTS

This work was supported by the Burroughs Wellcome Fund and The University of North Carolina School of Medicine grants to K.M.C., a training grant from the National Institutes of Health to R.T.D. (5-T32-GM007092-29), and a grant from the National Institutes of Health to O.S. (HL49277).

We thank Sylvia Hiller, Gleb Rozanov, Kirk McNaughton, and Kui Kwon Kim for technical assistance and Frank Conlon and Da-Zhi Wang for helpful advice and discussions.

REFERENCES

1. **Aiyar, N., K. Rand, N. A. Elshourbagy, Z. Zeng, J. E. Adamou, D. J. Bergsma, and Y. Li.** 1996. A cDNA encoding the calcitonin gene-related peptide type 1 receptor. J. Biol. Chem. **271:**11325–11329.
2. **Albertin, G., M. Rucinski, G. Carraro, M. Forneris, P. Andreis, L. K. Malendowicz, and G. G. Nussdorfer.** 2005. Adrenomedullin and vascular endothelium growth factor genes are overexpressed in the regenerating rat adrenal cortex, and AM and VEGF reciprocally enhance their mRNA expression in cultured rat adrenocortical cells. Int. J. Mol. Med. **16:**431–435.
3. **Allaker, R. P., and S. Kapas.** 2003. Adrenomedullin and mucosal defence: interaction between host and microorganism. Regul. Pept. **112:**147–152.
4. **Autelitano, D. J.** 1998. Cardiac expression of genes encoding putative adrenomedullin/calcitonin gene-related peptide receptors. Biochem. Biophys. Res. Commun. **250:**689–693.
5. **Caron, K. M., and O. Smithies.** 2001. Extreme hydrops fetalis and cardiovascular abnormalities in mice lacking a functional adrenomedullin gene. Proc. Natl. Acad. Sci. USA **98:**615–619.
6. **Chisaka, H., E. Morita, K. Murata, N. Ishii, N. Yaegashi, K. Okamura, and K. Sugamura.** 2002. A transgenic mouse model for non-immune hydrops fetalis induced by the NS1 gene of human parvovirus B19. J. Gen. Virol. **83:**273–281.
7. **Cornish, J., A. Grey, K. E. Callon, D. Naot, B. L. Hill, C. Q. Lin, L. M. Balchin, and I. R. Reid.** 2004. Shared pathways of osteoblast mitogenesis induced by amylin, adrenomedullin, and IGF-1. Biochem. Biophys. Res. Commun. **318:**240–246.
8. **Czyzyk, T. A., Y. Ning, M. S. Hsu, B. Peng, R. E. Mains, B. A. Eipper, and J. E. Pintar.** 2005. Deletion of peptide amidation enzymatic activity leads to edema and embryonic lethality in the mouse. Dev. Biol. **287:**301–313.
9. **Elshourbagy, N. A., J. E. Adamou, A. M. Swift, J. Disa, J. Mao, S. Ganguly, D. J. Bergsma, and N. Aiyar.** 1998. Molecular cloning and characterization of the porcine calcitonin gene-related peptide receptor. Endocrinology **139:** 1678–1683.
10. **Eva, C., and R. Sprengel.** 1993. A novel putative G protein-coupled receptor highly expressed in lung and testis. DNA Cell Biol. **12:**393–399.
11. **Fernandez-Sauze, S., C. Delfino, K. Mabrouk, C. Dussert, O. Chinot, P. M. Martin, F. Grisoli, L. Ouafik, and F. Boudouresque.** 2004. Effects of adrenomedullin on endothelial cells in the multistep process of angiogenesis: involvement of CRLR/RAMP2 and CRLR/RAMP3 receptors. Int. J. Cancer **108:**797–804.
12. **Fluhmann, B., R. Muff, W. Hunziker, J. A. Fischer, and W. Born.** 1995. A human orphan calcitonin receptor-like structure. Biochem. Biophys. Res. Commun. **206:**341–347.
13. **Gangula, P. R., H. Zhao, S. C. Supowit, S. J. Wimalawansa, D. J. Dipette, K. N. Westlund, R. F. Gagel, and C. Yallampalli.** 2000. Increased blood pressure in alpha-calcitonin gene-related peptide/calcitonin gene knockout mice. Hypertension **35:**470–475.
14. **Han, Z. Q., H. A. Coppock, D. M. Smith, S. Van Noorden, M. W. Makgoba, C. G. Nicholl, and S. Legon.** 1997. The interaction of CGRP and adrenomedullin with a receptor expressed in the rat pulmonary vascular endothelium. J. Mol. Endocrinol. **18:**267–272.
15. **Harrison, J. K., C. M. Barber, and K. R. Lynch.** 1993. Molecular cloning of a novel rat G-protein-coupled receptor gene expressed prominently in lung, adrenal, and liver. FEBS Lett. **318:**17–22.
16. **Ishimitsu, T., T. Nishikimi, Y. Saito, K. Kitamura, T. Eto, K. Kangawa, H. Matsuo, T. Omae, and H. Matsuoka.** 1994. Plasma levels of adrenomedullin, a newly identified hypotensive peptide, in patients with hypertension and renal failure. J. Clin. Investig. **94:**2158–2161.
17. **Iwasaki, H., S. Eguchi, M. Shichiri, F. Marumo, and Y. Hirata.** 1998. Adrenomedullin as a novel growth-promoting factor for cultured vascular smooth muscle cells: role of tyrosine kinase-mediated mitogen-activated protein kinase activation. Endocrinology **139:**3432–3441.
18. **Jougasaki, M., C. M. Wei, L. J. McKinley, and J. C. Burnett, Jr.** 1995. Elevation of circulating and ventricular adrenomedullin in human congestive heart failure. Circulation **92:**286–289.
19. **Juaneda, C., Y. Dumont, and R. Quirion.** 2000. The molecular pharmacology of CGRP and related peptide receptor subtypes. Trends Pharmacol. Sci. **21:**432–438.
20. **Kano, H., M. Kohno, K. Yasunari, K. Yokokawa, T. Horio, M. Ikeda, M. Minami, T. Hanehira, T. Takeda, and J. Yoshikawa.** 1996. Adrenomedullin as a novel antiproliferative factor of vascular smooth muscle cells. J. Hypertens. **14:**209–213.
21. **Kapas, S., K. J. Catt, and A. J. Clark.** 1995. Cloning and expression of cDNA encoding a rat adrenomedullin receptor. J. Biol. Chem. **270:**25344–25347.
22. **Kapas, S., and A. J. Clark.** 1995. Identification of an orphan receptor gene

as a type 1 calcitonin gene-related peptide receptor. Biochem. Biophys. Res. Commun. **217:**832–838.
23. **Karkkainen, M. J., P. Haiko, K. Sainio, J. Partanen, J. Taipale, T. V. Petrova, M. Jeltsch, D. G. Jackson, M. Talikka, H. Rauvala, C. Betsholtz, and K. Alitalo.** 2004. Vascular endothelial growth factor C is required for sprouting of the first lymphatic vessels from embryonic veins. Nat. Immunol. **5:**74–80.
24. **Kato, K., H. Yin, J. Agata, H. Yoshida, L. Chao, and J. Chao.** 2003. Adrenomedullin gene delivery attenuates myocardial infarction and apoptosis after ischemia and reperfusion. Am. J. Physiol. Heart Circ. Physiol. **285:** H1506–H1514.
25. **Kennedy, S. P., D. Sun, J. J. Oleynek, C. F. Hoth, J. Kong, and R. J. Hill.** 1998. Expression of the rat adrenomedullin receptor or a putative human adrenomedullin receptor does not correlate with adrenomedullin binding or functional response. Biochem. Biophys. Res. Commun. **244:**832–837.
26. **Kim, W., S. O. Moon, M. J. Sung, S. H. Kim, S. Lee, J. N. So, and S. K. Park.** 2003. Angiogenic role of adrenomedullin through activation of Akt, mitogen-activated protein kinase, and focal adhesion kinase in endothelial cells. FASEB J. **17:**1937–1939.
27. **Kitamura, K., K. Kangawa, M. Kawamoto, Y. Ichiki, S. Nakamura, H. Matsuo, and T. Eto.** 1993. Adrenomedullin: a novel hypotensive peptide isolated from human pheochromocytoma. Biochem. Biophys. Res. Commun. **192:**553–560.
28. **Kobayashi, K., K. Kitamura, N. Hirayama, H. Date, T. Kashiwagi, I. Ikushima, Y. Hanada, Y. Nagatomo, M. Takenaga, T. Ishikawa, T. Imamura, Y. Koiwaya, and T. Eto.** 1996. Increased plasma adrenomedullin in acute myocardial infarction. Am. Heart J. **131:**676–680.
29. **Kohno, M., T. Hanehira, H. Kano, T. Horio, K. Yokokawa, M. Ikeda, M. Minami, K. Yasunari, and J. Yoshikawa.** 1996. Plasma adrenomedullin concentrations in essential hypertension. Hypertension **27:**102–107.
30. **Koller, B. H., L. J. Hagemann, T. Doetschman, J. R. Hagaman, S. Huang, P. J. Williams, N. L. First, N. Maeda, and O. Smithies.** 1989. Germ-line transmission of a planned alteration made in a hypoxanthine phosphoribosyltransferase gene by homologous recombination in embryonic stem cells. Proc. Natl. Acad. Sci. USA **86:**8927–8931.
31. **Komatsu, Y., H. Shibuya, N. Takeda, J. Ninomiya-Tsuji, T. Yasui, K. Miyado, T. Sekimoto, N. Ueno, K. Matsumoto, and G. Yamada.** 2002. Targeted disruption of the Tab1 gene causes embryonic lethality and defects in cardiovascular and lung morphogenesis. Mech. Dev. **119:**239–249.
32. **Li, N., C. Y. Fang, Z. Z. Wang, Y. L. Wang, F. B. Wang, E. Gao, and G. X. Zhang.** 2004. Expression of calcitonin gene-related peptide type 1 receptor mRNA and their activity-modifying proteins in the rat nucleus accumbens. Neurosci. Lett. **362:**146–149.
33. **Livak, K. J., and T. D. Schmittgen.** 2001. Analysis of relative gene expression data using real-time quantitative PCR and the $2^{-\Delta\Delta CT}$ 0 method. Methods **25:**402–408.
34. **Lu, J. T., Y. J. Son, J. Lee, T. L. Jetton, M. Shiota, L. Moscoso, K. D. Niswender, A. D. Loewy, M. A. Magnuson, J. R. Sanes, and R. B. Emeson.** 1999. Mice lacking alpha-calcitonin gene-related peptide exhibit normal cardiovascular regulation and neuromuscular development. Mol. Cell. Neurosci. **14:**99–120.
35. **Macri, C. J., A. Martinez, T. W. Moody, K. D. Gray, M. J. Miller, M. Gallagher, and F. Cuttitta.** 1996. Detection of adrenomedullin, a hypotensive peptide, in amniotic fluid and fetal membranes. Am. J. Obstet. Gynecol. **175:**906–911.
36. **Majid, D. S., P. J. Kadowitz, D. H. Coy, and L. G. Navar.** 1996. Renal responses to intra-arterial administration of adrenomedullin in dogs. Am. J. Physiol. **270:**F200–F205.
37. **Malendowicz, L. K., M. T. Conconi, P. P. Parnigotto, and G. G. Nussdorfer.** 2003. Endogenous adrenomedullin system regulates the growth of rat adrenocortical cells cultured in vitro. Regul. Pept. **112:**27–31.
38. **McCright, B., X. Gao, L. Shen, J. Lozier, Y. Lan, M. Maguire, D. Herzlinger, G. Weinmaster, R. Jiang, and T. Gridley.** 2001. Defects in development of the kidney, heart and eye vasculature in mice homozygous for a hypomorphic Notch2 mutation. Development **128:**491–502.
39. **McLatchie, L. M., N. J. Fraser, M. J. Main, A. Wise, J. Brown, N. Thompson, R. Solari, M. G. Lee, and S. M. Foord.** 1998. RAMPs regulate the transport and ligand specificity of the calcitonin-receptor-like receptor. Nature **393:** 333–339.
40. **Miyashita, K., H. Itoh, N. Sawada, Y. Fukunaga, M. Sone, K. Yamahara, T. Yurugi, and K. Nakao.** 2003. Adrenomedullin promotes proliferation and migration of cultured endothelial cells. Hypertens. Res. **26**(Suppl.)**:**S93–S98.
41. **Murphy, T. C., and W. K. Samson.** 1995. The novel vasoactive hormone, adrenomedullin, inhibits water drinking in the rat. Endocrinology **136:**2459–2463.
42. **Nishio, K., Y. Akai, Y. Murao, N. Doi, S. Ueda, H. Tabuse, S. Miyamoto, K. Dohi, N. Minamino, H. Shoji, K. Kitamura, K. Kangawa, and H. Matsuo.** 1997. Increased plasma concentrations of adrenomedullin correlate with relaxation of vascular tone in patients with septic shock. Crit. Care Med. **25:**953–957.
43. **Niu, P., T. Shindo, H. Iwata, A. Ebihara, Y. Suematsu, Y. Zhang, N. Takeda, S. Iimuro, Y. Hirata, and R. Nagai.** 2003. Accelerated cardiac hypertrophy and renal damage induced by angiotensin II in adrenomedullin knockout mice. Hypertens. Res. **26:**731–736.
44. **Niu, P., T. Shindo, H. Iwata, S. Iimuro, N. Takeda, Y. Zhang, A. Ebihara, Y. Suematsu, K. Kangawa, Y. Hirata, and R. Nagai.** 2004. Protective effects of endogenous adrenomedullin on cardiac hypertrophy, fibrosis, and renal damage. Circulation **109:**1789–1794.
45. **Njuki, F., C. G. Nicholl, A. Howard, J. C. Mak, P. J. Barnes, S. I. Girgis, and S. Legon.** 1993. A new calcitonin-receptor-like sequence in rat pulmonary blood vessels. Clin. Sci. (London) **85:**385–388.
46. **Puri, M. C., J. Rossant, K. Alitalo, A. Bernstein, and J. Partanen.** 1995. The receptor tyrosine kinase TIE is required for integrity and survival of vascular endothelial cells. EMBO J. **14:**5884–5891.
47. **Salmon, A. M., I. Damaj, S. Sekine, M. R. Picciotto, L. Marubio, and J. P. Changeux.** 1999. Modulation of morphine analgesia in alphaCGRP mutant mice. Neuroreport **10:**849–854.
48. **Samson, W. K., and T. C. Murphy.** 1997. Adrenomedullin inhibits salt appetite. Endocrinology **138:**613–616.
49. **Shichiri, M., N. Fukai, N. Ozawa, H. Iwasaki, and Y. Hirata.** 2003. Adrenomedullin is an autocrine/paracrine growth factor for rat vascular smooth muscle cells. Regul. Pept. **112:**167–173.
50. **Suri, C., P. F. Jones, S. Patan, S. Bartunkova, P. C. Maisonpierre, S. Davis, T. N. Sato, and G. D. Yancopoulos.** 1996. Requisite role of angiopoietin-1, a ligand for the TIE2 receptor, during embryonic angiogenesis. Cell **87:**1171–1180.
51. **Tokudome, T., T. Horio, F. Yoshihara, S. Suga, Y. Kawano, M. Kohno, and K. Kangawa.** 2002. Adrenomedullin inhibits doxorubicin-induced cultured rat cardiac myocyte apoptosis via a cAMP-dependent mechanism. Endocrinology **143:**3515–3521.
52. **Tsuruda, T., M. Jougasaki, G. Boerrigter, L. C. Costello-Boerrigter, A. Cataliotti, S. C. Lee, L. Salz-Gilman, L. J. Nordstrom, C. G. McGregor, and J. C. Burnett.** 2003. Ventricular adrenomedullin is associated with myocyte hypertrophy in human transplanted heart. Regul. Pept. **112:**161–166.
53. **Tsuruda, T., J. Kato, K. Kitamura, M. Kawamoto, K. Kuwasako, T. Imamura, Y. Koiwaya, T. Tsuji, K. Kangawa, and T. Eto.** 1999. An autocrine or a paracrine role of adrenomedullin in modulating cardiac fibroblast growth. Cardiovasc. Res. **43:**958–967.
54. **Udono, T., K. Takahashi, M. Nakayama, O. Murakami, Y. K. Durlu, M. Tamai, and S. Shibahara.** 2000. Adrenomedullin in cultured human retinal pigment epithelial cells. Investig. Ophthalmol. Vis. Sci. **41:**1962–1970.
55. **Wang, X., L. Xue, and L. Tong.** 1999. Influence of vasoactive peptides on homocysteine-induced proliferation of cultured rabbit vascular smooth muscle cell. Zhonghua Yi Xue Za Zhi **79:**411–413. (In Chinese.)
56. **Wigle, J. T., and G. Oliver.** 1999. Prox1 function is required for the development of the murine lymphatic system. Cell **98:**769–778.
57. **Yin, H., L. Chao, and J. Chao.** 2004. Adrenomedullin protects against myocardial apoptosis after ischemia/reperfusion through activation of Akt-GSK signaling. Hypertension **43:**109–116.
58. **Zhang, L., A. O. Hoff, S. J. Wimalawansa, G. J. Cote, R. F. Gagel, and K. N. Westlund.** 2001. Arthritic calcitonin/alpha calcitonin gene-related peptide knockout mice have reduced nociceptive hypersensitivity. Pain **89:**265–273.